Holocephalan embryos provide evidence for gill arch appendage reduction and opercular evolution in cartilaginous fishes

J. Andrew Gillis[a,1], Kate A. Rawlinson[b], Justin Bell[c], Warrick S. Lyon[d], Clare V. H. Baker[a], and Neil H. Shubin[e,1]

[a]Department of Physiology, Development and Neuroscience, University of Cambridge, Cambridge CB2 3DY, United Kingdom; [b]Department of Genetics, Evolution and Environment, University College London, London, WC1E 6BT United Kingdom; [c]Department of Primary Industries, Marine and Freshwater Fisheries Resource Institute, Queenscliff, Victoria 3225, Australia; [d]National Institute of Water and Atmospheric Research, Hataitai, Wellington 6021, New Zealand; and [e]Department of Organismal Biology and Anatomy, University of Chicago, Chicago, IL 60637

Edited by Sean B. Carroll, University of Wisconsin, Madison, WI, and approved December 15, 2010 (received for review August 31, 2010)

Chondrichthyans possess endoskeletal appendages called branchial rays that extend laterally from their hyoid and gill-bearing (branchial) arches. Branchial ray outgrowth, like tetrapod limb outgrowth, is maintained by Sonic hedgehog (Shh) signaling. In limbs, distal endoskeletal elements fail to form in the absence of normal *Shh* signaling, whereas shortened duration of *Shh* expression correlates with distal endoskeletal reduction in naturally variable populations. Chondrichthyans also exhibit natural variation with respect to branchial ray distribution—elasmobranchs (sharks and batoids) possess a series of ray-supported septa on their hyoid and gill arches, whereas holocephalans (chimaeras) possess a single hyoid arch ray-supported operculum. Here we show that the elongate hyoid rays of the holocephalan *Callorhinchus milii* grow in association with sustained *Shh* expression within an opercular epithelial fold, whereas *Shh* is only transiently expressed in the gill arches. Coincident with this transient *Shh* expression, branchial ray outgrowth is initiated in *C. milii* but is not maintained, yielding previously unrecognized vestigial gill arch branchial rays. This is in contrast to the condition seen in sharks, where sustained *Shh* expression corresponds to the presence of fully formed branchial rays on the hyoid and gill arches. Considered in light of current hypotheses of chondrichthyan phylogeny, our data suggest that the holocephalan operculum evolved in concert with gill arch appendage reduction by attenuation of Shh-mediated branchial ray outgrowth, and that chondrichthyan branchial rays and tetrapod limbs exhibit parallel developmental mechanisms of evolutionary reduction.

Chondrichthyans are divided into two morphologically distinct lineages—the elasmobranchs (sharks, skates, and rays) and the holocephalans (chimaeras). One of the most striking morphological differences between these lineages is the distribution of branchial rays within their pharyngeal endoskeleton. Elasmobranchs possess branchial rays on their hyoid and gill arches (Fig. 1 *A–D*). These appendages extend beyond the limit of the primary gill lamellae, and support the interbranchial septa that sit between adjacent gill slits (1). Holocephalans, on the other hand, have been reported to possess branchial rays only on their hyoid arch (2) (Fig. 1 *E* and *F*), where they provide endoskeletal support for an operculum. Whether holocephalans have derived the operculate pharyngeal endoskeleton from an elasmobranch-like condition or vice versa has remained an open question for decades, due to strong discordance among hypotheses of stem-group phylogenetic relationships (2–8) and the absence of unequivocal branchial ray homologs outside of chondrichthyans.

Few Paleozoic chondrichthyan fossils preserve cartilaginous branchial rays. *Cladoselache* (9) and *Trystichius* (10) possessed branchial rays on their hyoid and gill arches—much like extant elasmobranchs—and both of these taxa have been resolved to the elasmobranch stem in different positions (3–7). This arrangement would reaffirm the primitive presence of hyoid and gill arch branchial rays in the elasmobranch crown group, but leaves the primitive condition for the chondrichthyan crown group unresolved. More extensive analyses, including exceptionally complete material of the stethacanthid *Akmonistion zangerli* (11), however, suggest an alternative placement of key ray-bearing taxa. These analyses resolve *Cladoselache* and the symmoriids (including the hyoid plus gill arch ray-bearing *Akmonistion*) as paraphyletic stem-group holocephalans (8, 11) (see also ref. 12), a topology that implies the reduction or loss of gill arch rays in holocephalans. More recently, a cladistic evaluation of several problematic "acanthodian" taxa resolved *Climatius* (13) and *Brochoadmones* (14)—both of which possessed septate gills—to the chondrichthyan stem (15). A scenario is therefore emerging in which septate gills (presumably branchial ray-supported) are plesiomorphic for the chondrichthyan crown group, with holocephalans having undergone reduction of their gill arch branchial rays coincident with the evolution of their hyoid ray-supported operculum (Fig. 2).

In vertebrate taxa that exhibit secondary loss or reduction of limbs, appendage outgrowth is often initiated but subsequently arrested, leaving behind vestiges of adult structures that were primitively present. This is seen, for instance, at the level of the hind limbs of some snakes (16, 17) and cetaceans (18, 19). It has been demonstrated in limbs that distal endoskeletal elements fail to form in the absence of normal Shh signaling (20, 21), and that shortened duration of *Shh* expression in the limb bud zone of polarizing activity correlates with distal endoskeletal reduction in lizards with naturally variable digit complements (22). Chondrichthyan branchial rays and limbs share a number of developmental features in common, including outgrowth mediated by a Shh-fibroblast growth factor (Fgf) feedback loop that operates within a specialized epithelial signaling center (23). With this in mind, we sought to test the hypothesis that holocephalans have undergone comparable gill arch branchial ray reduction by investigating pharyngeal endoskeletal development and signaling center activity in two key taxa—an elasmobranch shark (*Scyliorhinus canicula*) and a holocephalan (*Callorhinchus milii*).

Until now, comparative studies addressing the developmental basis of morphological differences between elasmobranchs and holocephalans have been hindered by the relative inaccessibility

Author contributions: J.A.G. designed research; J.A.G., K.A.R., J.B., and W.S.L. performed research; C.V.H.B. contributed new reagents/analytic tools; J.A.G. and N.H.S. analyzed data; and J.A.G., C.V.H.B., and N.H.S. wrote the paper.

The authors declare no conflict of interest.

This article is a PNAS Direct Submission.

Freely available online through the PNAS open access option.

Data deposition: The sequences reported in this paper have been deposited in the GenBank database [*Scyliorhinus canicula* Shh, partial coding sequence (cds) (accession no. HM991336), *Callorhinchus milii* Shh, partial cds (accession no. HM807523), and *C. milii* Ptc2, partial cds (accession no. HQ589326)].

[1]To whom correspondence may be addressed. E-mail: jag93@cam.ac.uk or nshubin@uchicago.edu.

This article contains supporting information online at www.pnas.org/lookup/suppl/doi:10.1073/pnas.1012968108/-/DCSupplemental.

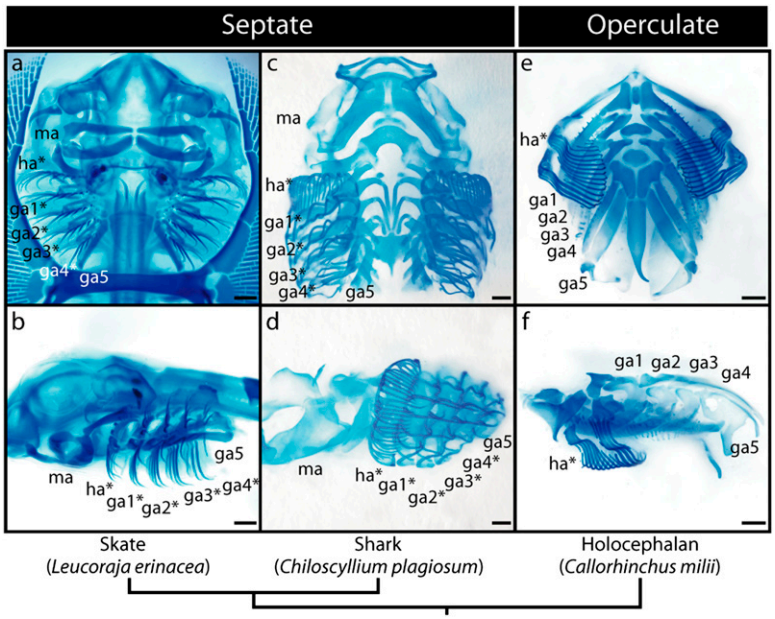

Fig. 1. Overview of chondrichthyan pharyngeal endoskeletal anatomy and branchial ray distribution. Visceral skeletal preparations of (*A* and *B*) the little skate (*Leucoraja erinacea*), (*C* and *D*) the white-spotted bamboo shark (*Chiloscyllium plagiosum*), and (*E* and *F*) a holocephalan *Callorhinchus milii* (mandibular arch removed). *A*, *C*, and *E* are ventral views (anterior to the top); *B*, *D*, and *F* are lateral views (anterior to the left). In each panel, branchial ray-bearing arches are indicated by an asterisk. ga1–5, gill arches 1–5; ha, hyoid arch; ma, mandibular arch. (Scale bars, 1 mm.)

of holocephalan embryos for molecular analysis. Guided by anecdotal data from recreational fishermen and fisheries biologists, we conducted SCUBA surveys of two *C. milii* oviposition sites—Westernport Bay in southeastern Australia, and Garnes Bay in Pelorus Sound, New Zealand (Figs. S1 and S2)—and we successfully recovered samples of *C. milii* eggs. These samples, along with more readily available embryos of *S. canicula*, formed the basis for a comparative study of elasmobranch and holocephalan pharyngeal skeletal development.

Results

We initially characterized the development and distribution of branchial rays in *S. canicula*. By stage (st.) 31 of *S. canicula* development, the hyomandibula and ceratohyal of the hyoid arch and the epibranchial and ceratobranchial components of gill arches 1–5 have formed (Fig. 3 *A–F*). Proximal primary branchial ray elements have formed within the hyoid arch (Fig. 3*A*), and outgrowth of branchial rays from the epi- and ceratobranchials of gill arches 1–4 has commenced (Fig. 3 *B–E*). By st. 32, a distal series of secondary branchial rays are forming within the hyoid arch (Fig. 3*G*), and these grow both proximally (in the direction of the primary rays) and distally into the septum of the hyoid arch. Branchial ray outgrowth continues from gill arches 1–4 (Fig. 3 *H–K*), whereas gill arch 5 remains devoid of branchial rays (Fig. 3*L*). At st. 34, the majority of the secondary branchial rays of the hyoid arch have fused proximally with the primary rays, giving rise to a forked cartilage pattern (Fig. 3*M*). The branchial rays that extend from gill arches 1–4, however, remain simple and rod-like. The ray distribution observed in *S. canicula* at st. 34—namely forked branchial rays extending from the hyoid arch (Fig. 3*M*), rod-like branchial rays extending from gill arches 1–4 (Fig. 3 *N–Q*), and no branchial rays extending from gill arch 5 (Fig. 3*R*)—persists posthatching and into adulthood. This ray distribution is also similar to the condition seen in batoid elasmobranchs (skates and rays) (24).

We next cloned a large fragment of *S. canicula Shh* and characterized its pharyngeal expression by in situ hybridization to determine how Shh signaling relates to branchial ray distribution in sharks (phylogenetic analysis of *Shh* sequences is presented in Fig. S3). *Shh* expression is detected in the pharyngeal arches of *S. canicula* at st. 29 (Fig. 4*A*), persists until st. 31 (Fig. 4*B*), and spans the entire dorsal-ventral extent of the hyoid and gill arch septa. Examination in section reveals that, in both the hyoid (Fig. 4*C*) and gill arches (Fig. 4*D*), *Shh* expression is restricted to the distal epithelium of each interbranchial septum. *Patched2* (*Ptc2*)—a receptor and downstream target of *Shh* signaling (25)—is expressed in the pharyngeal mesenchyme directly subjacent to the *Shh*-expressing epithelium in the hyoid (Fig. 4*E*) and first four gill arches (Fig. 4*F*). This indicates that the Shh signal that emanates from the distal pharyngeal epithelium is being transduced in pharyngeal mesenchyme. Sustained Shh signaling from pharyngeal epithelium to pharyngeal mesenchyme therefore correlates with branchial ray outgrowth from the hyoid and first four gill arches in *S. canicula*. The presence of this developmental feature in both shark and skate (23) suggests that this represents a primitive condition for the elasmobranch crown group.

An examination of pharyngeal endoskeletal development and *Shh* expression in the holocephalan *C. milii* reveals a condition that diverges considerably from that observed in *S. canicula*. At st. 29 of *C. milii* development, a proximal primary ray and a series of distal secondary rays have chondrified within the hyoid arch (Fig. 3*A*i). Histological examination (planes of section schematized in Fig. 5 *A* and *D*) show that these rays sit adjacent to the lamellae of the hyoid opercular hemibranch (Fig. 5*B*) and form underneath a distinctive epithelial fold that has formed along the leading edge of the outgrowing operculum (Fig. 5*C*). At this stage, we detect *Shh* expression along the entire dorsal-ventral extent of the hyoid and gill arches (Fig. 4*G*). Sections reveal that, in both the hyoid (Fig. 4*I*) and gill arches (Fig. 4*J*), *Shh* expression is restricted to the distal pharyngeal arch epithelium. Expression of *Ptc2* in the mesenchyme of the hyoid (Fig. 4*K*) and gill arches (Fig. 4*L*) indicates that, as in *S. canicula*, the epithelial Shh signal is transduced in subjacent pharyngeal mesenchyme. Although there are no gross morphological signs of branchial ray outgrowth from the gill arches at st. 29 (Fig. 3*Bi–Fi*), several foci of mesenchymal condensation are present along the posterior border of the ceratobranchials of gill arches 1–3 (Fig. 5*E*). These condensations are easily distinguished from the developing cartilaginous gill rakers (Fig. 5*E*). Because the position of these foci is comparable to the position at which the gill arch branchial rays form in elasmobranchs, we interpret these condensations as the initiation of gill arch branchial ray outgrowth.

At st. 31 of *C. milii* development, *Shh* and *Ptc2* expression is sustained in the epithelium and mesenchyme, respectively, of the hyoid arch operculum (Fig. 4 *H*, *M*, and *O*). However, *Shh* and *Ptc2* expression is no longer detected in the gill arches (Fig. 4 *H*,

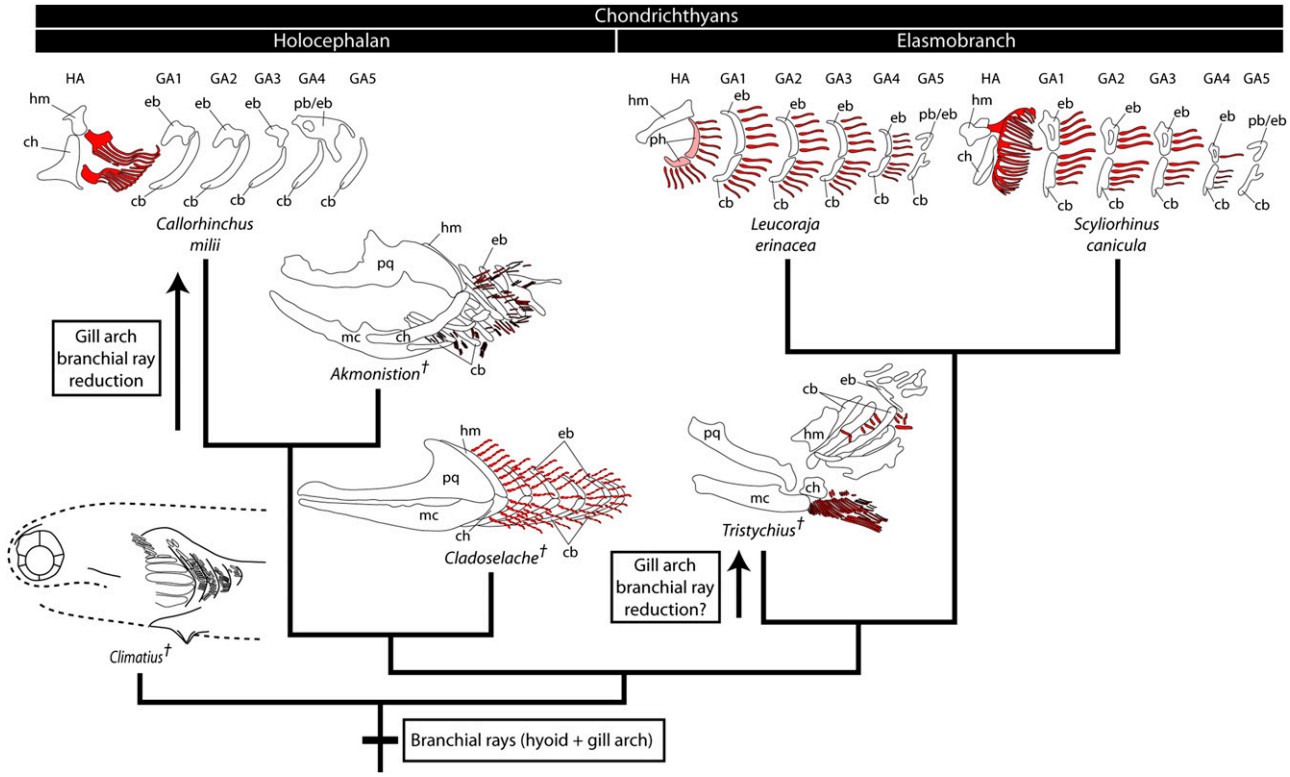

Fig. 2. Phylogeny of key chondrichthyan taxa and the evolution of branchial rays. Branchial rays (red) were primitively distributed on the hyoid plus gill arches of chondrichthyans, as inferred from their presence on the hyoid plus gill arches in the elasmobranch crown group (*L. erinacea*, *S. canicula*) and the holocephalan stem group (*Cladoselache*, *Akmonistion*). This is further supported by the presence of septate gills in *Climatius*, a putative stem chondrichthyan. This topology implies a reduction of gill arch branchial rays coincident with the evolution of the operculum in the holocephalan crown group (*C. milii*). *Trystichius*, with its elongate hyoid arch rays and short gill arch rays, may represent the independent reduction of gill arch branchial rays in an elasmobranch. Phylogeny is based on refs. 8, 11, and 15. *Akmonistion* was redrawn from ref. 11. *Cladoselache* was redrawn based on ref. 9. *Trystichius* was redrawn from ref. 10. *Climatius* was redrawn from ref. 13. cb, ceratobranchial; ch, ceratohyal; eb, epibranchial; GA1–5, gill arches 1–5; HA, hyoid arch; hm, hyomandibula; mc, Meckel's cartilage; pb/eb, compound pharyngobranchial/epibranchial; ph, pseudohyal; pq, palatoquadrate. †, fossil taxa.

N, and *P*). This expression pattern correlates with the continued outgrowth of branchial rays from the hyoid arch (Fig. 3*Gi*) and the absence of fully formed branchial rays from the gill arches (Fig. 3*Hi–Li*). A closer examination of gill arches 1–3 in a st. 36 *C. milii* embryo reveals a row of small, chondrified projections from the caudo-lateral face of the ceratobranchial element of each arch (Fig. 5*F*). These projections are morphologically distinct from the two rows of cartilaginous gill rakers that project rostro-laterally from the gill arches (Fig. 5*G*), and their position corresponds to the sites of mesenchymal condensation that were observed at st. 29. Given the relationship of these elements to the ceratobranchial, and their initial appearance in association with transient *Shh* expression in the gill arch epithelium, we interpret these structures as gill arch branchial rays whose outgrowth was initiated but not maintained.

Discussion

The morphological disparity exhibited by extant elasmobranchs and holocephalans has fueled much debate about the primitive versus derived nature of fundamental visceral endoskeletal characters in these taxa (2, 8, 12, 26–28). Until now, the relative inaccessibility of holocephalan embryos has hindered attempts to address these questions from a molecular developmental perspective. Our data demonstrate that the basic pattern of hyoid arch branchial ray chondrogenesis is shared between sharks and holocephalans, with one or more proximal primary rays fusing with distal secondary rays to yield a forked cartilage pattern. The holocephalan operculum, therefore, appears to have arisen not by major endoskeletal reorganization or novelty but rather by sustained Shh-mediated branchial ray outgrowth from the hyoid arch. In addition, we demonstrate the presence of previously unrecognized gill arch branchial rays in the holocephalan *C. milii*. In light of phylogenetic hypotheses that predict a loss or reduction of gill arch branchial rays along the holocephalan stem (8, 11, 12), we interpret these short rays as vestigial structures (29). That these vestiges form coincident with transient *Shh* expression in the gill arch pharyngeal epithelium of *C. milii* suggests that, as in the limbs of tetrapods (22), differences in the duration of *Shh* expression during appendage outgrowth may underlie endoskeletal variation in chondrichthyan branchial rays (Fig. S4).

The presence of vestigial gill arch rays in *C. milii* suggests that this example of evolutionary appendage reduction occurred by loss of one or more outgrowth maintenance factors, and not by failed initiation of outgrowth. In other vertebrate taxa, antagonism of repressive signals is a commonly used developmental mechanism for maintaining appendage outgrowth. In the tetrapod limb bud, tempered activity of Bone Morphogenetic Protein (Bmp) family members by BMP antagonists is crucial in maintaining feedback between the zone of polarizing activity and the apical ectodermal ridge. BMP signaling negatively regulates limb bud outgrowth by promoting apical ectodermal ridge regression (30, 31), and this effect is counteracted by Shh-dependent expression of the secreted BMP antagonist Gremlin (32, 33). A similar role for antagonist-modulated BMP signaling has been demonstrated in the developing mammalian genital tubercle (34). The outgrowth of chondrichthyan branchial rays also depends upon a feedback loop between Shh and FGF signaling (23), although nothing is currently known about the molecular players

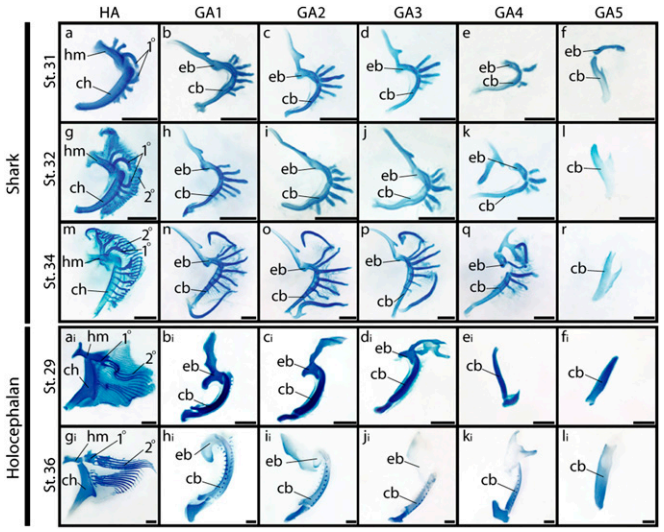

Fig. 3. A growth series of hyoid and gill arches in a shark, *S. canicula*, and a holocephalan, *C. milii*. Arches are dissected and oriented in frontal view. *S. canicula* at st. 31 (*A–F*), st. 32 (*G–L*), and st. 34 (*M–R*) shows the distribution of branchial rays on the hyoid arch and gill arches 1–4. Branchial rays are absent from gill arch 5. *C. milii* at st. 29 (*Ai–Fi*) and st. 36 (*Gi–Li*) shows prominent branchial rays on the hyoid arch, but lacks fully formed rays on the gill arches. Note that both *S. canicula* and *C. milii* possess branched branchial rays on their hyoid arches, resulting from the fusion of primary (proximal) and secondary (distal) hyoid rays. 1°, primary hyoid ray; 2°, secondary hyoid ray; cb, ceratobranchial; ch, ceratohyal; eb, epibranchial; hm, hyomandibula. (Scale bars, 1 mm.)

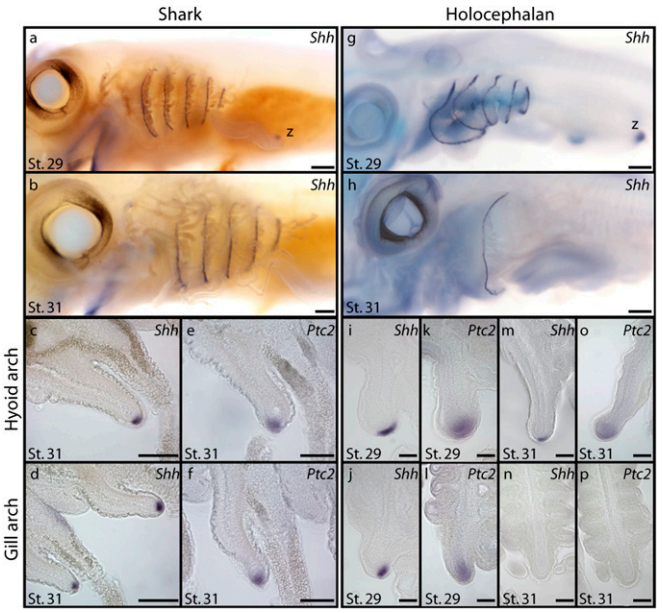

Fig. 4. *Shh* signaling correlates with branchial ray outgrowth in a shark, *S. canicula*, and a holocephalan, *C. milii*. (*A*) At st. 29 of *S. canicula* development, *Shh* is expressed in the hyoid arch and gill arches, and this expression pattern persists beyond (*B*) st. 31. Sections reveal that in *S. canicula*, *Shh* expression in the (*C*) hyoid and (*D*) gill arches is restricted to the distal pharyngeal epithelium, whereas *Ptc2* expression in the (*E*) hyoid and (*F*) gill arches is restricted to pharyngeal mesenchyme. (*G*) At st. 29 of *C. milii* development, *Shh* is expressed in the hyoid arch and gill arches. However, by (*H*) st. 31 of *C. milii* development, *Shh* expression persists only in the developing hyoid arch operculum. Sections reveal that at st. 29 of *C. milii* development, *Shh* expression in the (*I*) hyoid and (*J*) gill arches is restricted to the distal pharyngeal arch epithelium, whereas expression of *Ptc2* in the (*K*) hyoid and (*L*) gill arches is restricted to the pharyngeal mesenchyme. By st. 31, (*M*) *Shh* expression is maintained in the distal epithelium of the hyoid arch operculum, but is not detected in the (*N*) gill arch epithelium, and (*O*) *Ptc2* expression is maintained in the mesenchyme of the hyoid arch but is not detected in the (*P*) gill arches. Sustained *Shh* signaling in the hyoid arch and gill arches of *S. canicula* correlates with branchial ray outgrowth from the hyoid arch and gill arches 1–4. Similarly, sustained *Shh* expression in the hyoid arch only of *C. milii* correlates with sustained branchial ray outgrowth exclusively within the operculum. Note the expression of *Shh* in the zone of polarizing activity (z) of the pectoral fin in (*A*) *S. canicula* and (*G*) *C. milii*. [Scale bars, 250 μm (*A–H*) and 100 μm (*I–P*).]

that effect this cross-talk. Comparative investigation into the factors that maintain and terminate limb bud and branchial ray outgrowth may reveal that diverse vertebrate appendages exhibit not only shared mechanisms of outgrowth and patterning but also parallel developmental mechanisms of evolutionary reduction.

It is important to note that a scenario of hyoid arch ray expansion/gill arch ray reduction along the holocephalan stem likely does not address the total extent of branchial ray variation in chondrichthyans. Dick (10) reconstructed *Trystichius arcuatus* as possessing elongate hyoid arch rays that supported a functional operculum, as well as relatively short gill arch rays. As *Trystichius* consistently resolves to the elasmobranch stem (2, 4, 6–8), this likely represents the independent evolution of an operculum supported by elongate hyoid arch rays—and the independent reduction of gill arch branchial rays—in an elasmobranch (Fig. 2). There is evidence of hyoid arch branchial rays in the xenacanthiform *Orthacanthus* (35), although the nature of the gill arches in this taxon is not well known. A hyoid ray-supported opercular flap has been reported in the symmoriid *Falcatus* (36) (hyoid rays reported after reexamination in ref. 8), and has also been described in certain iniopterygians (37, 38), although there is evidence that these groups may be stem holocephalans (8, 11, 12, 39, 40). With such variation documented in only a small number of known taxa, a thorough reevaluation of chondrichthyan phylogeny and pharyngeal endoskeletal anatomy is clearly needed to accurately reconstruct the frequency, timing, and polarity of chondrichthyan branchial ray expansion and reduction.

A comparable reevaluation of pharyngeal endoskeletal anatomy in stem osteichthyans may also shed light on the origin and homology of the osteichthyan operculum. Like the chondrichthyan operculum, the osteichthyan operculum is derived from an outgrowth of the hyoid arch. However, the operculum of extant osteichthyans is not supported by endoskeletal branchial rays but rather by a series of dermal opercular bones and branchiostegal rays (41). A rudiment of this hyoid-derived operculum may even be present in amniote osteichthyans, as indicated by the brief period of Shh-associated outgrowth observed in the second arch of chicken embryos (23, 42). The hyoid operculum of osteichthyans and the hyoid/gill arch operculum/septa of chondrichthyans likely represent a case of convergent skeletal elements (intramembranous ossifications versus endoskeletal appendages, respectively) functioning to support a homologous embryonic hyoid arch outgrowth. The primitive condition for the gnathostome crown group—dermal versus endoskeletal support, and single operculate versus septate gills—remains to be determined.

Branchiostegal rays are present on the operculum of *Acanthodes* (a stem osteichthyan) and on the hyoid arch of *Climatius* (a stem chondrichthyan) (15), although the latter also appears to possess septate gills, much like elasmobranchs (13). The pharyngeal endoskeleton of *Climatius* is not known, and although it has been suggested that *Acanthodes* possessed endoskeletal branchial rays in its hyoid arch (43), this remains contentious. Gill ray-like cartilages are present in large numbers in the stem gnathostome *Euphanerops* (44), although their orientation relative to the branchial arches—and their homology with respect to chondrichthyan branchial rays—remains uncertain. It is therefore unclear whether endoskeletal branchial rays arose along the chondrichthyan stem,

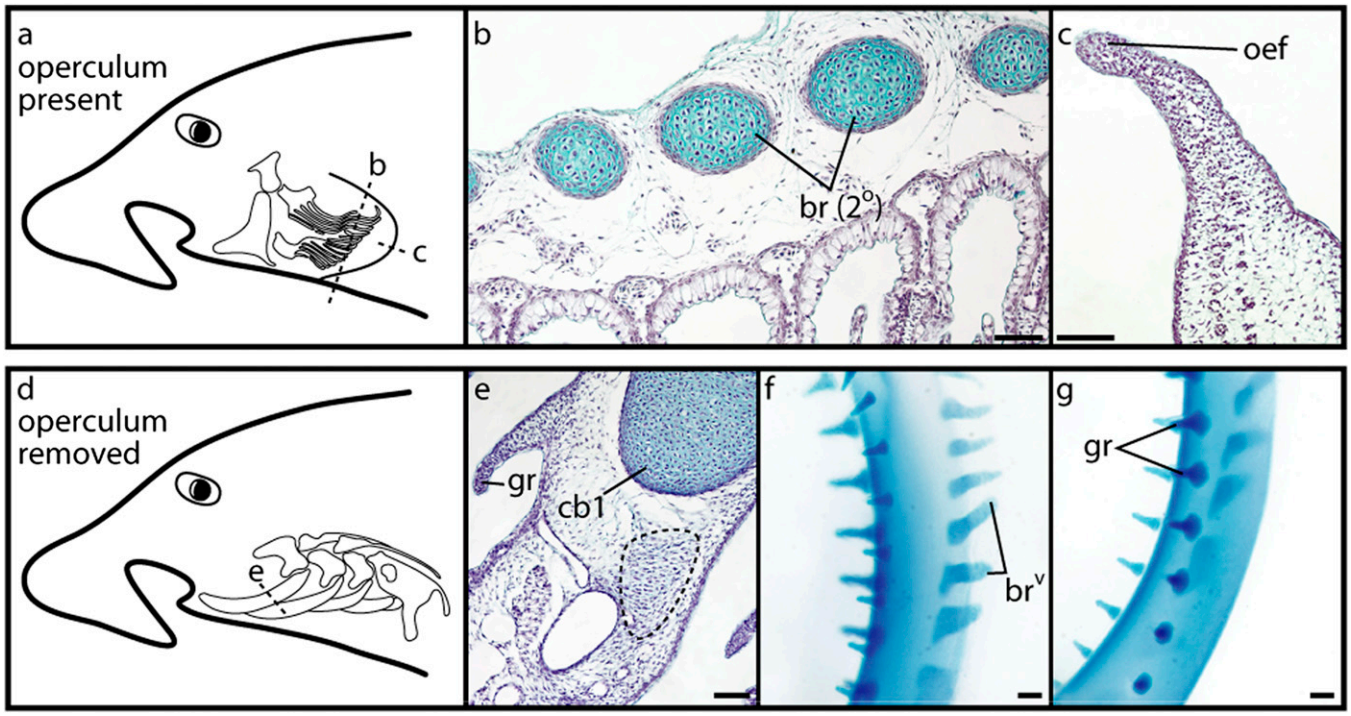

Fig. 5. Development of hyoid arch and vestigial gill arch branchial rays in a holocephalan, *C. milii*. (*A*) Schematic of the *C. milii* operculum skeleton in situ, illustrating planes of section in *B* and *C*. (*B*) A cross-section through the operculum of a st. 29 *C. milii* embryo shows secondary hyoid rays sitting adjacent to the hyoid arch hemibranch. (*C*) A horizontal section through the distal operculum of a st. 29 *C. milii* embryo shows the distinctive *Shh*-expressing epithelial fold that forms along the leading edge of the outgrowing operculum. (*D*) Schematic of the *C. milii* gill arch skeleton in situ, illustrating plane of section in *E*. (*E*) A cross-section through gill arch 1 of a st. 29 *C. milii* embryo shows a condensing branchial ray anlage (dashed line) extending caudo-laterally from the ceratobranchial. (*F*) A dissected ceratobranchial from gill arch 1 of a st. 36 *C. milii* embryo, in left lateral view, shows a single row of vestigial branchial rays extending caudo-laterally from the element. These vestigial rays are morphologically distinct from (*G*) the two rows of cartilaginous gill rakers that extend from the rostral face of the element. br (2°), secondary hyoid rays; br^{v}, vestigial branchial rays; cb1, ceratobranchial 1; gr, gill raker; oef, opercular epithelial fold. (Scale bars, 200 μm.)

or whether they were primitively present in gnathostome pharyngeal arches (perhaps in addition to dermal branchiostegal rays) and, if so, whether they were primitively distributed in the hyoid arch only, or on hyoid plus gill arches. These questions are fundamentally paleontological in nature. However, given the developmental mechanisms shared by branchial rays, fins, and limbs, resolving the origin and homology of gnathostome branchial rays will have significant bearing on hypotheses of the origin and evolution of other gnathostome appendages.

Methods

Collection and Staging of Embryos. Fixed embryos of the lesser-spotted dogfish/catshark, *Scyliorhinus canicula*, were obtained from the Centre National de la Recherche Scientifique Station Biologique in Roscoff, France (courtesy of Sylvie Mazan). *S. canicula* embryos were staged according to Ballard et al. (45). The embryo of the white-spotted bamboo shark, *Chiloscyllium plagiosum*, used in Fig. 1 was obtained from the John G. Shedd Aquarium in Chicago, IL (courtesy of Laura Hilstrom and Lise Christopher). Embryos of the elephant fish, *Callorhinchus milii*, were collected from the field in Westernport Bay, Victoria, Australia (Fig. S1) and Garnes Bay, New Zealand (Fig. S2). Eggs were collected by SCUBA. Before fixation, embryos were removed from their egg cases and euthanized with an overdose of MS-222 (ethyl 3-aminobenzoate methanesulfonate; Sigma-Aldrich) (1 g/L bath). Embryos for skeletal preparation and histology were fixed in 10% neutral buffered formalin at 4 °C, whereas embryos for mRNA in situ hybridization were fixed in modified Carnoy's fixative (three volumes 100% ethanol; three volumes 37% formaldehyde; one volume glacial acetic acid) at 4 °C. Following fixation, embryos were stored in 100% methanol at −20 °C. *C. milii* embryos were staged according to Didier et al. (46).

Skeletal Preparation, Histology, and mRNA in Situ Hybridization. Skeletal preparations and histology were conducted as described (24).

A 1,007-bp fragment of *S. canicula Shh* (GenBank accession no. HM991336) was amplified from total embryonic cDNA using the following degenerate primers: *ScShh*-Fwd 5′-AGYGGCAGATACGARGGSAAGAT-3′; *ScShh*-Rev 5′-AGGYGCYKGGAGTACCAGTGGA-3′. *S. canicula Ptc2* was amplified using gene-specific primers based on the available *S. canicula Ptc2* (GenBank accession no. EU814484). Fragments (844- and 849-bp) of *C. milii Shh* (GenBank accession no. HM807523) and *Ptc2* (GenBank accession no. HQ589326), respectively, were amplified from total embryonic cDNA using the following gene-specific primers [based on putative *Shh* and *Ptc2* sequences from the *C. milii* genome (47)]: *CmShh*-Fwd 5′-GCTGGCCTACAAGCAATACATCC-3′; *CmShh*-Rev 5′-CGAGATCTCCTCCAAGTAAACC-3′; *CmPtc2*-Fwd 5′-TTTCTGGCTCTGGGTATCGGTG-3′; *CmPtc2*-Rev 5′-GGTCTCACGAGGAACAATGTCTG-3′. Sequences were aligned and analyzed with Clustal W2 (48) and PHYLIP (49). Riboprobes were transcribed using T7 or Sp6 RNA polymerase (Promega) and digoxygenin-conjugated dUTPs (Roche) according to the manufacturers' protocols. mRNA in situ hybridization was carried out as described (50). *S. canicula* and *C. milii* whole-mount embryos were embedded in 15% gelatin and sectioned at 50 μm on a Leica VT1000S vibratome.

ACKNOWLEDGMENTS. We thank Sylvie Mazan for providing *S. canicula* embryos, and Mike Coates, Randy Dahn, Matt Friedman, Brian Hall, Dorit Hockman, and Melinda Modrell for discussions. We thank Terry Walker and Liz McGrath for facilitating the collection of *C. milii* embryos from the field in Australia. Fieldwork in New Zealand was funded by the National Geographic Society and Waitt Foundation grants program Grant W83-09 (to J.A.G.). Fieldwork in Australia was funded by grants from the University of Chicago Hinds Fund, the Australian Geographic Society, and the American Museum of Natural History Lerner-Gray Fund for Marine Research (to J.A.G.). J.A.G. was supported by a Smithsonian Link Foundation fellowship and a Newton International postdoctoral fellowship. N.H.S. was supported by funds from the Biological Sciences Division of the University of Chicago and The National Science Foundation. K.A.R. was supported by a Smithsonian Marine Science Network postdoctoral fellowship (Smithsonian Marine Station at Fort Pierce, contribution number 839).

1. Daniel JF (1934) *The Elasmobranch Fishes* (Univ of California Press, Berkeley), 3rd Ed.
2. Maisey JG (1984) Chondrichthyan phylogeny: A look at the evidence. *J Vert Paleont* 4: 359–371.
3. Schaeffer B, Williams M (1977) Relationships of fossil and living elasmobranchs. *Am Zool* 17:293–302.
4. Young GC (1982) Devonian sharks from South-Eastern Australia and Antarctica. *Palaeontology* 25:817–843.
5. Gaudin TJ (1991) A re-examination of elasmobranch monophyly and chondrichthyan phylogeny. *Neues Jahrb Geol Palaontol Abh* 182:133–160.
6. Maisey JG (2001) *Major Events in Early Vertebrate Evolution: Palaeontology, Phylogeny, Genetics and Development*, ed Ahlberg PE (Taylor and Francis, London), pp 263–288.
7. Lund R, Grogan ED (1997) Relationships of the Chimaeriformes and the basal radiation of the Chondrichthyes. *Rev Fish Biol Fish* 7:65–123.
8. Coates MI, Sequeira SEK (2001) *Major Events in Early Vertebrate Evolution: Palaeontology, Phylogeny, Genetics and Development*, ed Ahlberg PE (Taylor and Francis, London), pp 241–262.
9. Maisey JG (1989) Visceral skeleton and musculature of a Late Devonian shark. *J Vert Paleont* 9:174–190.
10. Dick JRF (1978) On the Carboniferous shark *Tristychius arcuatus* Agassiz from Scotland. *Trans R Soc Edinb* 70:63–109.
11. Coates MI, Sequeira SEK (2001) A new stethacanthid chondrichthyan from the Lower Carboniferous of Bearsden, Scotland. *J Vert Paleont* 21:438–459.
12. Janvier P (1996) *Early Vertebrates* (Oxford Univ Press, Oxford).
13. Miles RS (1973) Articulated acanthodian fishes from the Old Red Sandstone of England, with a review of the structure and evolution of the acanthodian shouldergirdle. *Bull Br Mus Nat Hist (Geol)* 24:111–213.
14. Hanke GF, Wilson MVH (2006) Anatomy of the Early Devonian acanthodian *Brochoadmones milesi* based on nearly complete body fossils, with comments on the evolution and development of paired fins. *J Vert Paleont* 26:526–537.
15. Brazeau MD (2009) The braincase and jaws of a Devonian 'acanthodian' and modern gnathostome origins. *Nature* 457:305–308.
16. Raynaud A (1985) *Biology of the Reptilia*, eds Gans C, Billett F (John Wiley and Sons, New York), Vol 15, pp 59–148 Development B.
17. Cohn MJ, Tickle C (1999) Developmental basis of limblessness and axial patterning in snakes. *Nature* 399:474–479.
18. Bejder L, Hall BK (2002) Limbs in whales and limblessness in other vertebrates: Mechanisms of evolutionary and developmental transformation and loss. *Evol Dev* 4: 445–458.
19. Thewissen JG, et al. (2002) Developmental basis for hindlimb loss in dolphins and origin of the cetacean bodyplan. *Proc Natl Acad Sci USA* 103:8414–8418.
20. Ros MA, et al. (2003) The chick *oligozeugodactyly* (*ozd*) mutant lacks Sonic hedgehog function in the limb. *Development* 130:527–537.
21. Stopper GF, Wagner GP (2007) Inhibition of Sonic hedgehog signaling leads to posterior digit loss in *Ambystoma mexicanum*: Parallels to natural digit reduction in urodeles. *Dev Dyn* 236:321–331.
22. Shapiro MD, Hanken J, Rosenthal N (2003) Developmental basis of evolutionary digit loss in the Australian lizard Hemiergis. *J Exp Zoolog B Mol Dev Evol* 297:48–56.
23. Gillis JA, Dahn RD, Shubin NH (2009) Shared developmental mechanisms pattern the gill arch and paired fin skeleton of vertebrates. *Proc Natl Acad Sci USA* 106: 5720–5724.
24. Gillis JA, Dahn RD, Shubin NH (2009) Chondrogenesis and homology of the visceral skeleton in the little skate, *Leucoraja erinacea* (Chondrichthyes: Batoidea). *J Morphol* 270:628–643.
25. Pearse RV II (2001) Vogan KJ, Tabin CJ (2001) *Ptc1* and *Ptc2* transcripts provide distinct readouts of Hedgehog signaling activity during chick embryogenesis. *Dev Biol* 239: 15–29.
26. de Beer GR, Moy-Thomas JA (1935) On the skull of Holocephali. *Phil Trans Roy Soc B* 224:287–312.
27. Grogan ED, Lund R, Didier D (1999) Description of the chimaerid jaw and its phylogenetic origins. *J Morphol* 239:45–59.
28. Maisey JG (2008) The postorbital palatoquadrate articulation in elasmobranchs. *J Morphol* 269:1022–1040.
29. Hall BK (2003) Descent with modification: The unity underlying homology and homoplasy as seen through an analysis of development and evolution. *Biol Rev Camb Philos Soc* 78:409–433.
30. Niswander L, Martin GR (1993) FGF-4 and BMP-2 have opposite effects on limb growth. *Nature* 361:68–71.
31. Pizette S, Niswander L (1999) BMPs negatively regulate structure and function of the limb apical ectodermal ridge. *Development* 126:883–894.
32. Zúñiga A, Haramis AP, McMahon AP, Zeller R (1999) Signal relay by BMP antagonism controls the SHH/FGF4 feedback loop in vertebrate limb buds. *Nature* 401:598–602.
33. Khokha MK, Hsu D, Brunet LJ, Dionne MS, Harland RM (2003) Gremlin is the BMP antagonist required for maintenance of Shh and Fgf signals during limb patterning. *Nat Genet* 34:303–307.
34. Suzuki K, et al. (2003) Regulation of outgrowth and apoptosis for the terminal appendage: External genitalia development by concerted actions of BMP signaling [corrected]. *Development* 130:6209–6220.
35. Hotton N III (1952) Jaws and teeth of American Xenacanth sharks. *J Paleontol* 26: 489–500.
36. Lund R (1985) The morphology of *Falcatus falcatus* St. John & Worthen, a Mississippian stethacanthid chondrichthyan from the Bear Gulch Limestone of Montana. *J Vert Paleont* 5:1–19.
37. Zangerl R, Case GR (1973) Iniopterygia: A new order of chondrichthyan fishes from the Pennsylvanian of North America. *Fieldiana Geol Mem* 6:1–67.
38. Grogan ED, Lund R (2009) Two new iniopterygians (Chondrichthyes) from the Mississippian (Serpukhovian) Bear Gulch Limestone of Montana with evidence of a new form of chondrichthyan neurocranium. *Acta Zool* 90(Suppl 1):134–151.
39. Pradel A, et al. (2009) Skull and brain of a 300-million-year-old chimaeroid fish revealed by synchrotron holotomography. *Proc Natl Acad Sci USA* 106:5224–5228.
40. Stahl BJ (1999) *Handbook of Paleoichthyology*, ed Schultze H-P (Pfeil, Munich), Vol 4, pp 1–163.
41. de Beer GR (1937) *The Development of the Vertebrate Skull* (Clarendon, Oxford).
42. Wall NA, Hogan BL (1995) Expression of bone morphogenetic protein-4 (BMP-4), bone morphogenetic protein-7 (BMP-7), fibroblast growth factor-8 (FGF-8) and Sonic hedgehog (SHH) during branchial arch development in the chick. *Mech Dev* 53: 383–392.
43. Jarvik E (1980) *Basic Structure and Evolution of Vertebrates* (Academic, London).
44. Janvier P, Arsenault M (2007) The anatomy of *Euphanerops longaevus* Woodward, 1900, an anaspid-like jawless vertebrate from the Upper Devonian of Miguasha, Quebec, Canada. *Geodiversitas* 29:143–216.
45. Ballard WW, Mellinger J, Lechenault H (1993) A series of normal stages for development of *Scyliorhinus canicula*, the lesser spotted dogfish (Chondrichthyes: Scyliorhinidae). *J Exp Zool* 267:318–336.
46. Didier DA, LeClair EE, Vanbuskirk DR (1998) Embryonic staging and external features of development of the chimaeroid fish, *Callorhinchus milii* (Holocephali, Callorhinchidae). *J Morphol* 236:25–47.
47. Venkatesh B, et al. (2007) Survey sequencing and comparative analysis of the elephant shark (*Callorhinchus milii*) genome. *PLoS Biol* 5:e101.
48. Larkin MA, et al. (2007) Clustal W and Clustal X version 2.0. *Bioinformatics* 23: 2947–2948.
49. Felsenstein J (1989) PHYLIP—Phylogeny inference package (version 3.2). *Cladistics* 5: 164–166.
50. O'Neill P, McCole RB, Baker CVH (2007) A molecular analysis of neurogenic placode and cranial sensory ganglion development in the shark, *Scyliorhinus canicula*. *Dev Biol* 304:156–181.